On Chip Counting and Localisation of Magnetite Pollution Nanoparticles

Siming Zuo[1], Jiuge Chen[1], Hua Fan[2], Rami Ghannam[1] and Hadi Heidari[1]
[1] Microelectronics Lab (meLAB), School of Engineering, University of Glasgow, G12 8QQ, UK
[2] State Key Laboratory of Electronic Thin Films and Integrated Devices, School of Electronic Science and Engineering, University of Electronic Science and Technology of China, Chengdu, China
hadi.heidari@glasgow.ac.uk

***Abstract*— Magnetic nanoparticles are generally smaller than 200 nm and can easily enter the human brain through the respiratory system. The harm that such nanoparticles can cause may lead to the loss of human life. This paper focuses on the modelling and simulation of a new kind of magnetic sensor, which can detect and localize these magnetite nanoparticles. The proposed sensors can help prevent these nanoparticles from polluting the environment, which will undoubtedly reduce their adverse risks to humans. The modelled magnetic sensor consists of a tunnelling magnetoresistive sensor, a conducting line, and magnetite nanoparticles. The localization and quantization of the magnetic nanoparticles can be realised by analysing different output voltages of the TMR sensor.**

Keywords*— *Magnetic Sensors; CMOS, Magnetite; Modelling; FEM Simulation.

I. Introduction

The volume of airborne particulate matter (PM) has been increasing significantly over the last two decades [1]. PM is a general term that accounts for all solid and liquid particles that are released into the atmosphere. These particles are separated by different variegated chemical compositions and sizes. For example, PM10 refers to the particles with the maximum equivalent aerodynamic diameter of 10 μm, while some other particles are smaller than 2.5 μm in diameter like PM2.5 [2]. Meanwhile, the increasing pollution nanoparticles in the air also include magnetite pollution particles with the diameter smaller than 200 nm. These magnetite nanoparticles can easily enter into the human brain through the respiratory system. The unique combination of redox activities where the surface charge and strong magnetic behaviour of the magnetite nanoparticles will have a strong influence on the human brain, thereby endangering human health and causing cancers [3]. The traditional devices are based on the weight and laser scattering detection, which are expensive and not portable. Therefore, it is important to develop a precise, repeatable and achievable remote monitoring technique.

This paper presents a simulation work based on finite element method using commercial software COMSOL, in which a magnetic sensor for accurate and repeated detection of magnetite pollution particle of dimension smaller than 200 nm has been simulated. The proposed sensing scheme relies a tunnelling magnetoresistive (TMR) sensor [4], shown in Fig. 1. The current applied to the conducting line will produce a magnetic field on the TMR sensor and magnetite nanospheres. Besides, the magnetized magnetite nanospheres will generate a stray field to the TMR sensor, which has a linear response to an external field. An output voltage is displayed to indicate the change in resistance due to these two magnetic fields. In other words, the different output voltages are used to simultaneously detect the position and number of magnetite nanoparticles on the chip [5].

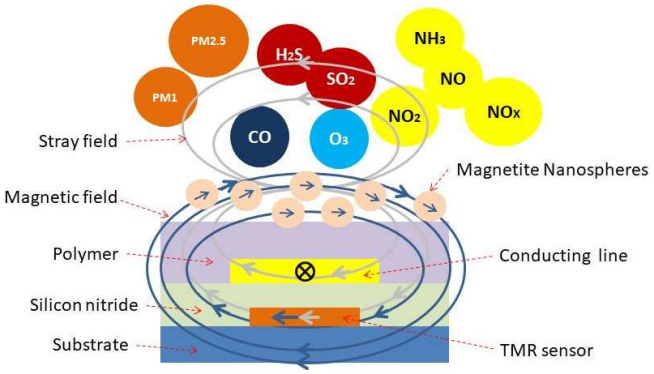

Fig. 1. Scheme of the magnetic sensing method showing the PM particles above the sensor.

II. Magnetic Sensors for Air Pollution Monitoring

In order to monitor magnetite nanoparticles, several different techniques have been proposed in the past few years. Table I summarises the basic information of the different air PM monitoring sensors.

The typical method is to use optical monitoring sensors, such as Alphasense OPC-N2, PPD42NS, PPD20V, and PPD60PV. However, the Alphasense OPC-N2 is a mature device with minimal maintenance and can only detect particles with the diameter larger than 0.38 μm [6]. The PPD42NS, PPD20V and PPD60PV sensors that are designed by Shinyei Technology can measure particles of around 500 nm in size [7]. However, a clean line of sight is needed for measurements. Therefore, they are unrealistic in the specific industrial environment like a coal combustion-based boiler.

The other method based on the on-chip CMOS monolithic capacitive sensor is shown in [2]. This chip makes use of a 32-channel lock-in architecture with dust collection area interdigitated differential microelectrodes and fabricated with the top metal and directly exposed to air. In the microcapacitor,

TABLE I: DIFFERENT TECHNOLOGIES OF AIR MONITORING

	JSSC [2]	Alphasense [8]	Shinyei [9]	This Work
Sensing Tech.	Capacitive	Optics	Optics	Magnetics
Particle Size	1–30 μm	380 nm	500 nm	50-200 nm

the dielectric constant of the interposed air volume is changed when the particles are deposited between two microelectrodes. Regarding this design, it can measure particles from 1 μm to 30 μm in diameter.

Even though these methods are high quality, the detected particles are still not small enough because the diameter of magnetite pollution particles is generally smaller than 200 nm. Over the last several decades, various magnetic sensors have been evaluated [3-7]. Among them, the TMR has the highest sensitivity to detect the ultra-low magnetic field. In this work, a TMR array will be employed for accurate counting and localisation of magnetite nanoparticles. Fig. 2 shows the basic structure consisting of free layer/barrier/pinned layer, and its transfer curve. The TMR with a bias voltage may exhibit electrical conducting properties and its electrical resistance varies as a linear function of the magnetic field strength over a certain field range due to the dependence of the tunnelling probability on the relative orientation of the magnetization in the two ferromagnetic (FM) layers [10]. The largest resistance value is obtained when the FM layers have an antiparallel orientation (R_{AP}). The lowest value occurs for a parallel orientation (R_P). The TMR is defined as the ratio [11]:

$$TMR = \frac{R_{AP} - R_P}{R_P} \tag{1}$$

For an ideal magnetic sensor, the transfer curve (Fig. 2 (a)) is linear and hysteresis-free within the intended field operating range. The curve possesses two stable resistance plateaus and a linear reversible path between them. Saturation fields (H_{sat}) define the ideal linear range ($2H_{sat}$) of the device, where a *dR* variation corresponds to a single *dH* value. It is important to point out that when the magnetizations are at a perpendicular angle, the resistance is at a median between R_{AP} and R_P. This is often an ideal angle and field for the "operating point" of a sensor because of the linear behaviour at this point. In other words, the MTJ will have a linear response to an external field only if the free layer magnetization changes its direction trough

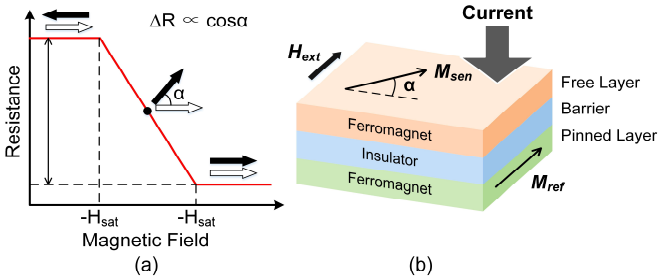

Fig. 2. TMR transfer curve principle. (a) R(H) linear behaviour and typical magnetization orientations correspondence; (b) current perpendicular-to-plane configuration for tunnel-magnetoresistive sensing.

coherent rotation. To achieve this behaviour, free and pinned layer magnetizations are set orthogonal to each other and the external magnetic field is applied perpendicular to the free layer but parallel to the pinned one.

In this paper, the TMR sensor is modelled in the state-of-the-art structure CoFeB/MgO/CoFeB [12] to ensure that the high magnetoresistance ratio provide higher output changes. It is a remarkable fact that the properties of the materials such as electrical conductivity, coercivity, relative permeability and relative permittivity can be measured in experiments and the parameters are only for the simulation purpose [12].

III. STRUCTURE AND MODELLING

A. COMSOL Structure

The simulation model is built in COMSOL, consisting of a cylinder model box, a conducting line, superparamagnetic particles and a TMR sensor array. Specifically, the cylinder model box with a radius of 20 μm is set in the air. The conducting line is copper with 15 μm, 6 μm and 0.3 μm in length, width and thickness respectively. The TMR sensor a "sandwich" structure based on ferromagnetic spin tunnelling junctions consisting of ferromagnetic–insulator–ferromagnetic layers. Here, materials are permalloy, nickel, and iron magnetic alloy, with 15 μm, 3 μm and 0.3 μm in length, width and thickness respectively. In addition, the superparamagnetic particles are Fe_2O_3 with a radius of 1.4 μm. Finally, the current applied to the conducting line is set to 30 mA.

Furthermore, in this study, the geometry of the TMR is defined as a tetrahedral mesh of user-defined size, dividing the 3D structures into small elements. It is used to estimate the current distribution in the MTJ devices with different strength of magnetic field and to account for possible geometrical mismatches. The computational mesh results in a system of ~10^8 tetrahedral finite element with an average element size of 2 nm in the multilayer.

B. Model Formulation

In order to simulate the magnetic field produced by the applied current in the conducting line, a physical field "*Magnetic Fields*" is added in the whole domain, while the "*Magnetic Fields No Currents*" physical field is used to simulate the magnetic field produced by magnetized superparamagnetic particles. This model is based on the Ampere's Law in a static case [3], which is

$$\nabla \times \left(\mu^{-1} \nabla \times \boldsymbol{A} \right) = \boldsymbol{J} \tag{2}$$

However, there exists crosstalk noise generated by the capacitive and inductive coupling between the TMR sensor and the conducting line, which will affect the output of the sensor voltage [6]. The crosstalk noise can be expressed as

$$V_{ct} = A_{ct} \cos\left(2\pi f_s t\right) \tag{3}$$

where the A_{ct} is the amplitude of the crosstalk noise signal and f_s is the operating frequency of the TMR sensor. Sometimes the crosstalk noise is larger than signals produced by magnetite

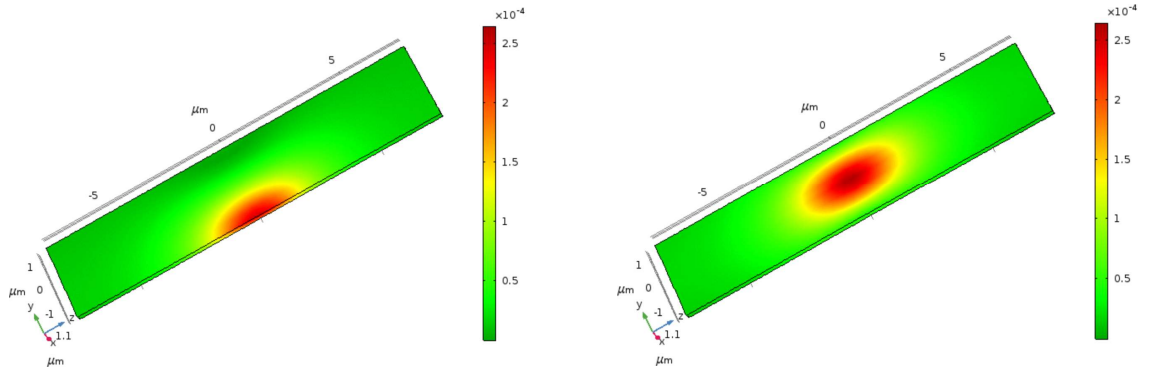

Fig. 3. The Y component of magnetic flux density in the stray field produced by the magnetite particles on the surface of a single TMR sensor.

particles. Therefore, it is necessary to utilize the frequency modulation to reduce this effect. Here, a lock-in amplifier is implemented to detect original signals within the crosstalk noise.

The currents applied to the conducting line and the TMR

$$I_M(t) = \sqrt{2} I_M \cos(2\pi f_M t) \tag{4}$$

$$I_S(t) = \sqrt{2} I_S \cos(2\pi f_S t) \tag{5}$$

where the I_M/I_S is the RMS applied current, and f_M/f_S is the corresponding operating frequency.

Due to the magnetic field produced by magnetization current and the stray field produced by the magnetized superparamagnetic particles [4], the resistance of the TMR element will be changed as

$$\Delta R(t, \mathrm{B}) = \sqrt{2} R_0 \delta B \cos(2\pi f_M t) \tag{6}$$

where R_0 and δ are the original internal resistance and sensitivity of the TMR sensor respectively, and B is total magnetic flux density produced by the current and the superparamagnetic particles.

The output of the TMR sensor thus can be calculated as

$$\begin{aligned} V(t, \mathrm{B}) &= I_S(t)(R_0 + \Delta R) + V_{ct1} + V_{ct2} \\ &= \left(\sqrt{2} I_S R_0 + A_{ct1}\right) \cos(2\pi f_S t) + A_{ct2} \cos(2\pi f_M t) \\ &\quad + I_S R_0 \delta B \cos(2\pi (f_S - f_M) t) \\ &\quad + I_S R_0 \delta B \cos(2\pi (f_S + f_M) t) \end{aligned} \tag{7}$$

where A_{ct1} and A_{ct2} are amplitudes of the crosstalk noise in different operating frequencies, f_S and f_M.

As explained before, the lock-in amplifier will detect the operation frequency at f_S and f_M respectively. Due to the current phases will not affect output results of the lock-in amplifier, they are negligible [7].

Finally, the output voltage is calculated by

$$V_{out} = V_M + V_{Bead} = \frac{1}{2\sqrt{2}} I_S R_0 \delta \left(\overline{B_M} + \overline{B_{Stray}}\right) \tag{8}$$

where $\overline{B_M}$ and $\overline{B_{Stray}}$ are average values of the magnetic flux density in the magnetization field and in the stray field.

IV. SIMULATION RESULTS AND DISCUSSION

Fig. 3 shows the Y component of the magnetic flux density of the stray field produced by the magnetite particles on the surface of the TMR sensor, which is the first step to achieve the localization of the magnetite nanoparticles.

During the movement of magnetite nanoparticles, the output voltages in the X and Y axes are shown in Fig. 4. The average output voltages are 33.426 μV at -3.7 μm and 34.97 μV at -1.7 μm, when the particles are moving along the X-axis. Therefore, the sensitivity of the output voltage is increased from 28 nV/μm at -3.7 μm to 176 nV/μm at -1.7 μm when the magnetite nanoparticles move per 0.1μm. When the magnetite nanoparticles are moving along the Y-axis, the average output voltages are 33.368 μV and 34.97 μV at edges and middle of the TMR sensor respectively. The sensitivity of the output voltage is changed from 2 nV/μm at the middle to 26 nV/μm at the edges when magnetite nanoparticles move per 0.1 μm. As expected, the stray field increases when the magnetite nanoparticles move near to the conducting line, causing an increase in the output voltage.

The structure of a nine TMR sensor array was modelled in COMSOL. The annulus around the sensors determines to an infinite area, which avoids error on the boundary of this structure.

The localization of the magnetite nanoparticles is shown in Fig. 5(a). It demonstrates the magnetic flux density of the stray field produced by the magnetite nanoparticles on the surface of the TMR sensor array.

In order to detect the number and position of the magnetite nanoparticles, the output voltage of each TMR sensor needs to be measured. When the particles are moving along the right three sensors (No.3, 6 and 9), Z-axis is remained constant at 20 μm while Y-axis is changed from -10 μm to +10 μm.

The output voltage of each sensor is shown in Fig. 5(b). It shows that the sensors No. 3, 6 and 9 lines have significant changes, while the other output voltages almost keep constant values. When the particles move to -10 μm, V_{total9} is the largest one. When the particles move to around 0 μm, the V_{total6} reach the maximum. V_{total3} is increased to the largest value when the particles move to +10 μm.

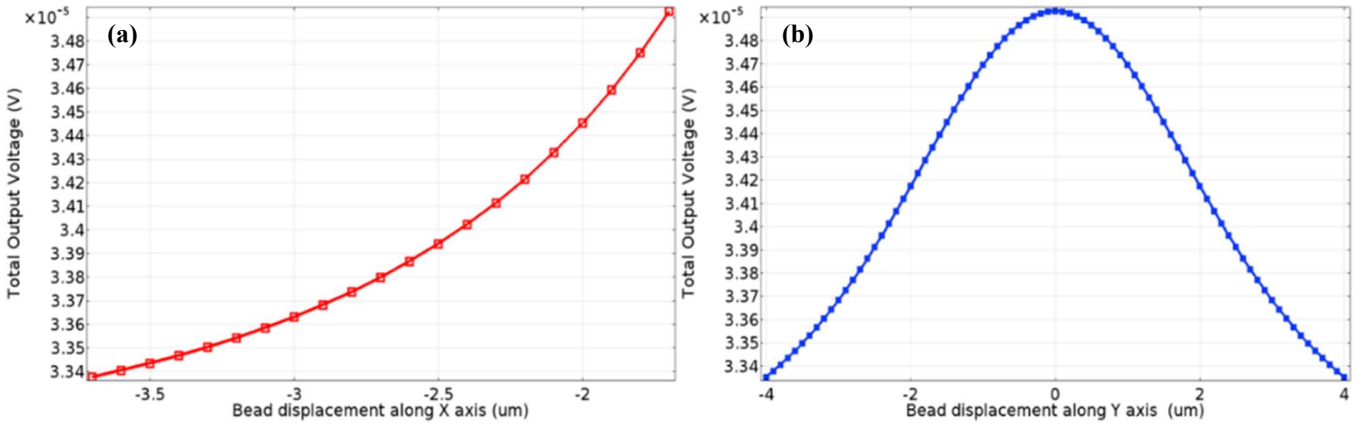

Fig. 4. The Output voltage of the TMR sensor when the magnetite particles are moving in (a) the X direction and (b) the Y direction.

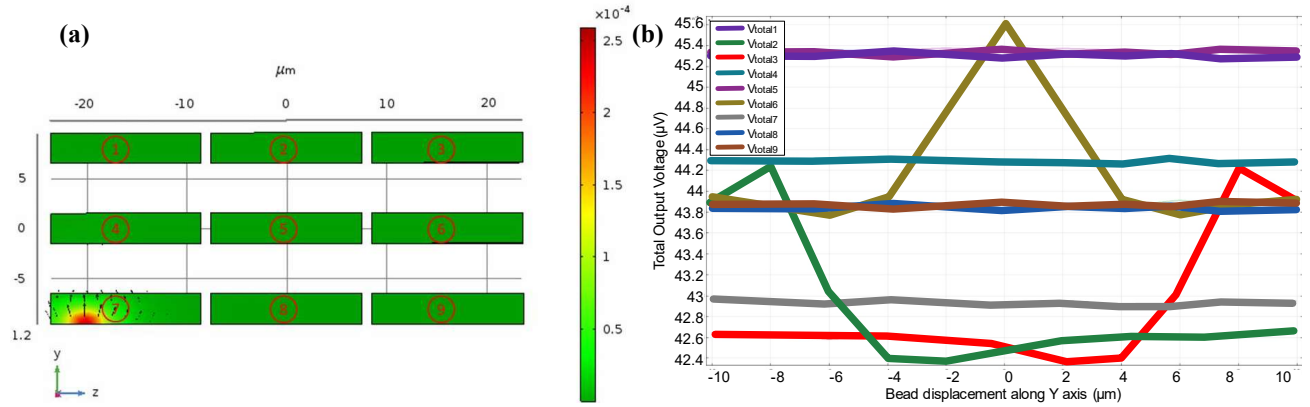

Fig. 5. (a) The Y component of magnetic flux density in the stray field produced by the magnetite particles on the surface of a 3×3 TMR sensor array; (b) The output voltage of each sensor when the magnetite particles are moving along the Y axis, keeping Z axis in a constant value (+20 μm).

V. Conclusion

This paper describes a new airborne particulate matter monitoring method with a TMR sensor array for localization and quantization of the pollution nanoparticles. When applying an alternating current to the conducting line, the produced magnetic field will attract the magnetite particles to the trapping well. Subsequently, the attracted magnetite particles will be magnetized by the magnetic field and then produce an external stray field. Both magnetic field and stray field will change the resistance of the TMR sensors. The different positions of magnetite particles will lead to different output voltages.

Finally, the output voltage of the TMR sensor array changed between 33.4 μV and 34.9 μV. With an advanced analogue frond-end circuit including amplifier, filter, and analog-to-digital converter, this small change will be shown and analyzed by the computer. Instead of existing commercial air monitoring sensors based on optical and chemical sensing technologies, this magnetic sensing technology can detect 50-200 nm magnetite particles, which turns magnetic sensing technology into a possibility. The results are promising for utilizing in the future monitoring of air pollution nanoparticles.

Acknowledgment

The authors acknowledge support of the Royal Society under grant "MAGLAB" RSG\R1\180269".

References

[1] C. I. Davidson, R. F. Phalen, and P. A. Solomon, "Airborne particulate matter and human health: a review," *Aerosol Sci. Technol.*, vol. 39, no. 8, pp. 737–749, 2005.

[2] P. Ciccarella, M. Carminati, M. Sampietro, and G. Ferrari, "Multichannel 65 zF rms resolution CMOS monolithic capacitive sensor for counting single micrometer-sized airborne particles on chip," *IEEE J. Solid-State Circuits*, vol. 51, no. 11, pp. 2545–2553, 2016.

[3] B. A. Maher *et al.*, "Magnetite pollution nanoparticles in the human brain," *Proc. Natl. Acad. Sci.*, vol. 113, no. 39, pp. 10797–10801, 2016.

[4] F. Li and J. Kosel, "A magnetic biosensor system for detection of E. coli," *IEEE Trans. Magn.*, vol. 49, no. 7, pp. 3492–3495, 2013.

[5] H. Heidari, E. Bonizzoni, U. Gatti, and F. Maloberti, "A 0.18-μm CMOS current-mode hall magnetic sensor with very low bias current and high sensitive front-end," in *SENSORS, 2014 IEEE*, 2014, pp. 1467–1470.

[6] "Alphasense Particle Monitor." [Online]. Available: http://www.alphasense.com/index.php/products/optical-particle-counter/.

[7] "SHINYEI Technology." [Online]. Available: http://www.shinyei.co.jp/stc/eng/optical/main_ppd60pv.html.

[8] H. Heidari, E. Bonizzoni, U. Gatti, and F. Maloberti, "A current-mode CMOS integrated microsystem for current spinning magnetic hall sensors," *Proc. - IEEE Int. Symp. Circuits Syst.*, pp. 678–681, 2014.

[9] H. Heidari, N. Wacker, S. Roy, and R. Dahiya, "Towards bendable CMOS magnetic sensors," in *Ph. D. Research in Microelectronics and Electronics (PRIME), 2015 11th Conference on*, 2015, pp. 314–317.

[10] M. Tondra, J. M. Daughton, D. Wang, R. S. Beech, A. Fink, and J. A. Taylor, "Picotesla field sensor design using spin-dependent tunneling devices," *J. Appl. Phys.*, vol. 83, no. 11, pp. 6688–6690, 1998.

[11] M. Julliere, "Tunneling between ferromagnetic films," *Phys. Lett. A*, vol. 54, no. 3, pp. 225–226, 1975.

[12] P. P. Freitas, R. Ferreira, and S. Cardoso, "Spintronic Sensors," *Proc. IEEE*, vol. 104, no. 10, pp. 1894–1918, 2016.